ROBUST MEAN ESTIMATION FOR REAL-TIME BLANKING IN RADIOASTRONOMY

Philippe Ravier[1], *Cedric Dumez-Viou*[1−2]

[1]Laboratory of Electronics, Signals, Images, Polytech'Orléans - University of Orleans
12, rue de Blois, BP 6744 Cedex 2, F-45067 Orléans, France
[2]Observatoire de Paris/(CNRS No.704), Station de radioastronomie, F-18330 Nançay, France
phone: + (33).2.38.49.48.63, fax: + (33).2.38.41.72.45, email: Philippe.Ravier@univ-orleans.fr
web: www.obs-nancay.fr/rfi

ABSTRACT

Radio astronomy observations suffer from strong interferences that need to be blanked both in the time and frequency domains. In order to achieve real-time computations, interference detection is made by simple thresholding. The threshold value is linked to the mean estimation of the power of clean observed data that follows a χ^2 distribution. Spurious values insensitivity is obtained by replacing mean by robust mean. A theoretical study of the variance of three estimators of the mean is presented. The study leads to a practical trimmed percentage that is chosen for the robust mean.

1. INTRODUCTION

Radioastronomy benefits from protected bands for the study of radio-sources. However, useful information is sometimes only available in bands occupied by telecommunication users. In those cases, signals of interest (SOI) are generally polluted by strong radio frequency interferences (RFI). Observation is still possible if a receiver is designed to handle high dynamic signals composed of weak SOI with superimposed strong RFI. Then, signal processing make RFI mitigation possible to retrieve the SOI.

Such a receiver is one of the current projects at the Nançay Observatory [1]. Robust Radio Receiver (R^3) can connect to 3 instruments (Nançay Radio Telescope, Nançay Decameter Array, Surveillance Antenna) and process up to 8 independent bands ranging from 875 kHz to 14 MHz bandwidth that can be combined to provide a larger band of analysis. This band can be channelized into 64 to 8192 subbands. Either Blackman windowing or 49152-coefficients polyphase filter can be used for FFT apodisation. RFI mitigation procedures can be applied in time and/or frequency domain, *i.e.* before and/or after FFT calculation. Current implementations are based on a robust threshold power detector. They allow real-time RFI mitigation : interference rejection is processed while observation is running.

For long time exposure, noise power probability density function (PDF) is assumed to be Gaussian. However RFI mitigation may require high time resolution. The Gaussian assumption does not hold anymore and the exact PDF must be taken into account for precise threshold derivation.

2. PROCEDURE USED FOR REAL-TIME

In order to achieve real-time computation, a simple thresholding drives the time and/or frequency blanking decision.

The problem is formulated as the following binary hypothesis test:

$$\begin{cases} H0: \text{ the SOI only is present,} \\ H1: \text{ the SOI is polluted with additive interference.} \end{cases}$$

The SOI is supposed to be Gaussian. On the other hand, no *a priori* information about the interference PDF is available. Nevertheless, the interference is usually powerful compared to the SOI. So the decision of blanking is made according to the false alarm probability (P_{fa}) that may be acceptable by the radio astronomers. The compromise for a good rejection of the interferences is to give up the smallest number of the highest values of the observations without compromising clean data with residual RFI. In practice, the P_{fa} is taken between 0.1% and 0.0001%. One solution to make the decision concerning the hypothesis testing problem is to compare the observation to a threshold: the $H0$ hypothesis is realized when the observation is smaller than the threshold. The $H1$ hypothesis is realized in the other case. When $H0$ is realized, the threshold value is updated with the new observation input. When $H1$ is realized, the blanking decision is made and the threshold value remains unchanged.

The threshold is calculated for a desired P_{fa}. Theoretical values may be derived when the PDF is known. Since the SOI is Gaussian, the power of the observation follows a χ^2 distribution in both time and frequency domains. Assuming the SOI follows a $\mathcal{N}(0,\sigma^2)$ distribution, the observation results in the sum of ν squared SOI independent realizations. The $\chi^2(\nu)$ cumulative distribution function may be written as an incomplete normalized Gamma function P :

$$F_{\chi^2(\nu)}(x) = P\left(\frac{\nu}{2}, \frac{x}{2}\right),$$

where the function P is defined as

$$P(\nu,x) = \frac{\Gamma(\nu,x)}{\Gamma(\nu)} = \frac{1}{\Gamma(\nu)} \int_0^x t^{\nu-1} e^{-t} dt$$

The Nançay Radio Observatory is the Unité scientifique de Nançay of the Observatoire de Paris, associated as Unité de Service et de Recherche No. 704 to the French Centre National de la Recherche Scientifique (CNRS).

The Nançay Observatory also gratefully acknowledges the financial support of the Conseil Régional de la Région Centre in France.

The work of C. Dumez-Viou was financially supported by Observatoire de Paris and by the European Social Fund.

and $\Gamma(\nu) = \Gamma(\nu, +\infty)$ is the Gamma function [2]. Given an admissible false alarm rate $P_{fa} = \alpha$ leads to the following value $threshold = 2\sigma^2 P^{-1}\left(\frac{\nu}{2}, 1-\alpha\right)$ where P^{-1} is the inverse tabulated P function. However, the variance σ^2 of each SOI realization is not precisely known and that value fluctuates over time due to changes in signal transmission (antenna position, ionosphere properties, ...). Since the mean value $\mu_{\chi^2(\nu)}$ of a $\chi^2(\nu)$ pdf equals $\nu\sigma^2$, the threshold is finally estimated as:

$$threshold = 2\frac{\widehat{\mu}_{\chi^2(\nu)}}{\nu} P^{-1}\left(\frac{\nu}{2}, 1-\alpha\right) \quad (1)$$

The key point therefore relies on a good estimation of the mean value of the power of the data that has to be RFI-mitigated. Different estimators have been computed in time and/or frequency domains for the best detection possible fitting the nature of the interferences.

2.1 Time Blanking

Time blanking needs to detect aberrant points, with real-time constraints. The input data are the real part and imaginary part of the complex-demodulated band-shifted received data. Time blanking is processed on the waveform that holds the instantaneous power of the received data. In this case, the thresholding procedure involves estimating the mean $\widehat{\mu_x}$ of independent realizations following $\chi^2(2)$ distributions. Online computation naturally leads to an adaptive way for the estimation of $\widehat{\mu_x}$ with respect to time:

$$\widehat{\mu_x}[t] = \widehat{\mu_x}[t-1] + \varepsilon \cdot (x[t] - \widehat{\mu_x}[t-1])$$

The waveform is computed as $x[t] = x_Q^2[t] + x_I^2[t]$. The components $x_Q[t]$ and $x_I[t]$ follow a centered Gaussian distribution with unknown variance σ^2. The time $t-1$ stands for the acquisition time of the samples preceding the current one. The choice of ε is a compromise between a short time response, a low variance of the mean estimator and RFI insensitivity.

First, a short settling time of the estimator is required to perform RFI mitigation as soon as possible after the beginning of the acquisition sequence. Then, the mean estimator is unbiased and the small value of ε corresponds to a reduced variance of the estimator since $Var(\widehat{\mu_x}) = 2\varepsilon\sigma^4$ (with σ^2 generally weak). Finally, RFI insensitivity is achieved by using a time constant longer than RFI events. For example, specifications of ground-based aviation radars give a pulse rate frequency of T_o = 1 ms for the emitted signal. On the R^3 receiver, ε is set to 0.00012 resulting in a settling time of 2-3 T_o.

Note that when interference is detected, the mean estimator value is not updated with the new sample in order to prevent the estimation to be polluted by incoherent values. The last computed estimator is kept unchanged. This time blanking procedure is real-time operational in the R^3 instrument at the front-end part of the spectrum analyser. Its use for radar blanking allows to freely observe in the highly corrupted bands occupied by radars (Figure 1).

2.2 Frequency Blanking

For scientific analysis purposes, time-frequency maps are computed on the fly: an averaged periodogram is estimated based on 50% overlapped temporal slices. Beyond weighting functions, the spectrum analyser offers two degrees of freedom for the computation of the power spectral density (PSD): the FFT length ranging from N=64 to N=4096 and the number of accumulations A (from 2^0 to 2^{17}) generating the average PSD. Each periodogram is computed as $|X_i(f)|^2$ with $X_i(f)$ being the FFT of the i^{th} temporal slice.

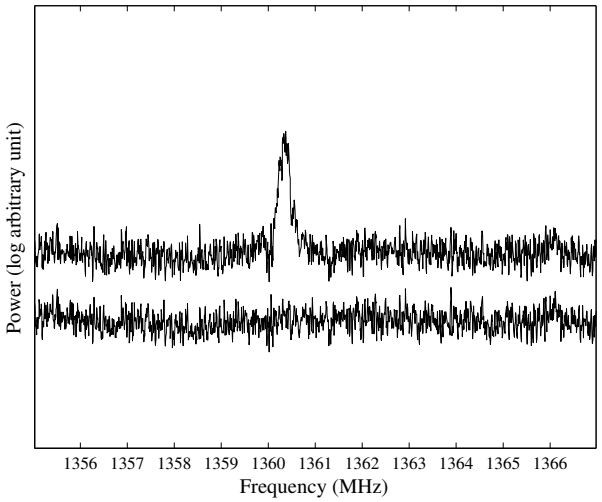

Figure 1: Illustration of sky noise background observation without (top) and with (bottom) radar blanking using the Nançay Radio Telescope. Time-exposure of 40s. The curves are shifted for display purpose.

The resulting estimator writes:

$$P(f) = \sum_{i=1}^{A} |X_i(f)|^2$$

so that $P(f)$ follows a $\chi^2(\nu)$ with $\nu = 2A$ varying from 2^1 to 2^{18} degrees of freedom. Note that the average periodogram theoretically rescales $P(f)$ by $\frac{1}{A}$. This stage is performed *a posteriori* for implementation constraints.

A frequency blanking procedure is applied each time a PSD is estimated. The threshold procedure is applied on the whole PSD. The threshold calculus (1) therefore holds, however the mean $\widehat{\mu}$ is estimated on the PSD samples.

Nevertheless, the mean of the PSD may be strongly corrupted, due to some channels that may be occupied by RFI polluters. The median estimator may be preferred instead. The problem is the computation cost of such an estimator as well as its deviation to the desired mean when the distribution is asymmetric (*i.e.* for low ν values). Another solution relies on robust mean estimators such as the trimmed mean or the Winsorized mean.

In the following part, we compare the mean estimator of the threshold value with the robust mean and the median estimators.

3. ROBUST ESTIMATION OF THE MEAN

For an easy comparison, we hereafter give the bias and variance of each estimator. The comparison will help choosing

the suitable parameters for the retained method.

3.1 The mean estimator

The reference mean estimator in (1) is theoretically expressed as the expectation of the $P(f)$ distribution:

$$\mu_{MN} = E\{P(f)\} = \nu\sigma^2$$

Let us estimate μ_{MN} by:

$$\widehat{\mu}_{MN} = \frac{1}{N}\sum_{f=1}^{N} P(f)$$

This classical estimator is consistent with the number of Fourier coefficients N since the estimator is unbiased with variance $2\nu\sigma^4/N$ and the $P(f)$ distribution is supposed to be white.

3.2 The median estimator

Let us note the theoretical median of $P(f)$ as:

$$\mu_{MD} = median_{f\in R}\{P(f)\} = 2\sigma^2 P^{-1}\left(\frac{\nu}{2},\frac{1}{2}\right).$$

The median is estimated on N values:

$$\widehat{\mu}_{MD} = median_{f=1\ldots N}\{P(f)\}.$$

The bias and variance of this estimator needs to derive the law of an order statistics for a $\chi^2(\nu)$ parent distribution. The k-moments of the median estimator are expressed as:

$$\begin{aligned} E\left\{\widehat{\mu}_{MD}^k\right\} &= K_N\int_0^1\left[2\sigma^2 P^{-1}\left(\frac{\nu}{2},\frac{u}{2}\right)\right]^k u^{\frac{N}{2}-1}(1-u)^{\frac{N}{2}}du, \\ \text{with } K_N &= \frac{N}{2}\frac{\Gamma(N+1)}{(\Gamma(N/2+1))^2} \end{aligned}$$

The bias and variance are numerically computed.

Figure 2 shows that the estimator becomes unbiased with the number of channels N growing and degree of freedom ν growing. The bias for low N values is actually negligible.

3.3 The trimmed mean estimator

The trimmed mean, like the median, is insensitive to spurious data or outliers. The trimmed mean is the mean computed after the q smallest observations and the q largest observations in the sample are deleted.

Considering $P_\delta(f)$ the δ trimmed distribution of $P(f)$. The parameter $\delta = q/N$ is the percentage of trimmed values at each side. The theoretical trimmed estimator writes:

$$\begin{aligned} \mu_{MR}(\delta) &= E\{P_\delta(f)\} \\ &= \nu\sigma^2\frac{P(\frac{\nu}{2}+1,\frac{b}{2}) - P(\frac{\nu}{2}+1,\frac{a}{2})}{F(b,\nu)-F(a,\nu)} \end{aligned}$$

The parameters a and b correspond to the low and high δ trimmed values of the $\chi^2(\nu)$ PDF:

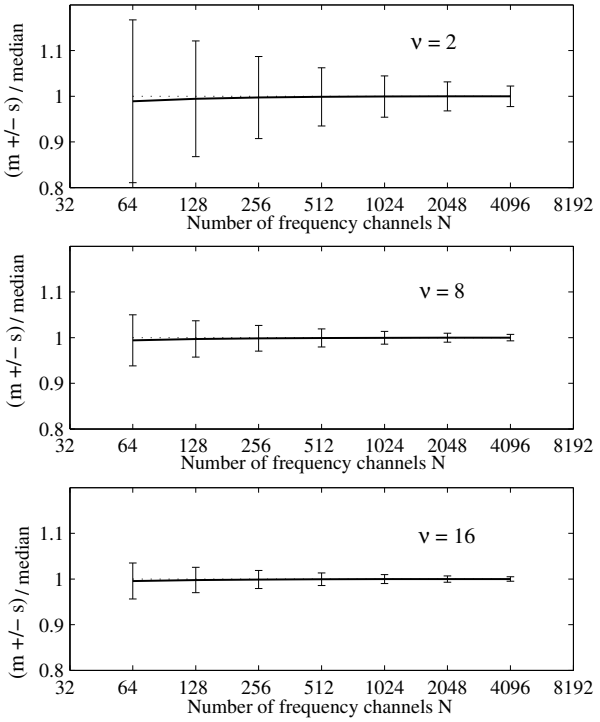

Figure 2: Mean and standard deviation for the median estimator (normalized with respect to the true median) for ν=2, 8 and 16.

$$\begin{aligned} a &= 2\sigma^2 P^{-1}(\frac{\nu}{2},\delta) \\ b &= 2\sigma^2 P^{-1}(\frac{\nu}{2},1-\delta) \end{aligned}$$

The function $F(x,\nu)$ stands for the $\chi^2(\nu)$ cumulative distribution function. Note that $\mu_{MR}(0) = \mu_{MN}$. Identically, we have $\mu_{MR}(\delta) \overset{\delta\to 0.5}{\to} \mu_{MD}$. Let us note $P^{(i)}$ the i^{th} order statistic of $P(f)$ when the data are arranged in increasing order. The δ trimmed mean is estimated by

$$\widehat{\mu}_{MR}(\delta) = \frac{1}{N-2q}\sum_{i=q+1}^{N-q} P^{(i)}, \quad \text{with } q = \lfloor \delta N \rfloor$$

The variance of this estimator approximately writes:

$$Var\{\widehat{\mu}_{MR}(\delta)\} \cong \frac{\nu^2\sigma^4}{N-2q}.$$
$$\frac{\left[P(\frac{\nu}{2}+2,\frac{b}{2}) - P(\frac{\nu}{2}+2,\frac{a}{2})\right] - \left[P(\frac{\nu}{2}+1,\frac{b}{2}) - P(\frac{\nu}{2}+1,\frac{a}{2})\right]^2}{[F(b,\nu)-F(a,\nu)]}$$

4. DISCUSSION

Figure 3 (top) shows the bias of estimation of the robust estimators with respect to the desired mean value μ_{MN}. Since the

$\widehat{\mu}_{MR}(\delta)$ estimators are unbiased with respect to their theoretical values, the bias of $\widehat{\mu}_{MR}(\delta)$ lies between 0 (case $\delta = 0$, equivalent to μ_{MN}) and 30 % that is the bias for $\widehat{\mu}_{MD}$ (case $\delta \to 0.5$). A normalized bias with respect to μ_{MN} is represented: its value rapidly falls with an increasing degree of freedom. Note that the normalized bias is independent of the window length N.

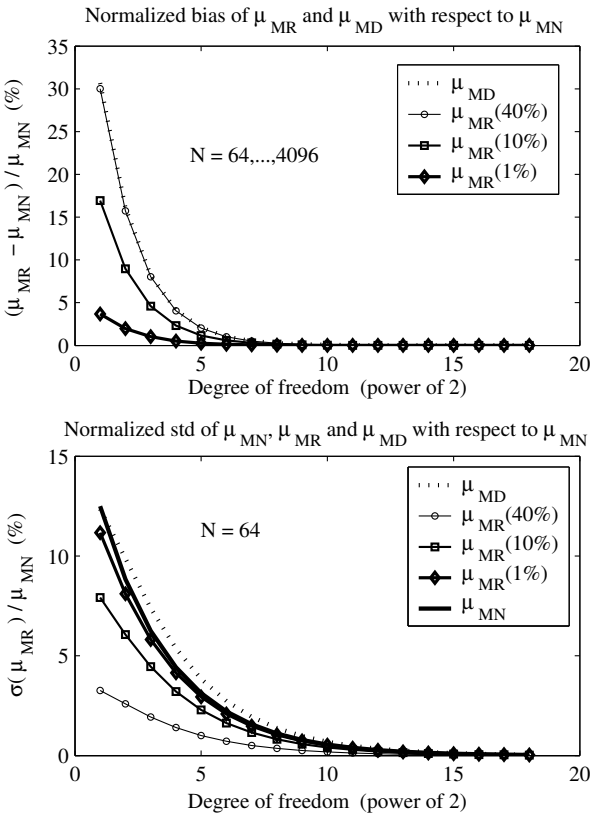

Figure 3: Normalized bias (top) and standard deviation (bottom) for the mean, median, and trimmed mean estimators.

The smallest value $N = 64$ yields the highest normalized standard deviation as shown figure 3 (bottom). The $\widehat{\mu}_{MD}$ estimator is the poorest. However it does not exceed 12.5 % of normalized standard deviation. The $\widehat{\mu}_{MD}$ estimator is slightly better. The normalized standard deviation of $\widehat{\mu}_{MR}(\delta)$ tends towards zero with an increasing value of δ. This is not surprising since the pdf becomes narrower and narrower when the trimmed parameter δ increases. When δ tends to 0.5, the samples are more and more confined between two certain values around the median value: the standard deviation of the trimmed pdf decreases (although the samples number becomes smaller). On the other hand, the $\widehat{\mu}_{MD}$ estimator has a completely different pdf that depends on order statistics showing bad performances in terms of standard deviation of the estimator.

In practice, a high trimmed value is preferable for sake of robustness with respect to RFI. The normalized standard deviation is therefore weak. The counterpart is the important bias with respect to μ_{MN} for low degrees of freedom.

As an example, the observed normalized bias of 27 % actually produces an error which is as big as taking 0.01 % instead of 0.0001 % in the false alarm probability, when accumulating 16 spectra (ν=32).

This mistake may be overcome by calculating a corrected trimmed mean. The trimmed values can be numerically computed in order to make the PDF symmetric such that the corrected trimmed mean equals the mean. The q' largest observations and the q'' smallest observations are deleted such that $\delta = (q' + q'')/2N$ is the average percentage of trimmed values and both the PDF and the trimmed PDF share the same first moment (Figure 4). These constraints yield to solve the nonlinear system with the two unknown quantities a' and b'

$$\begin{cases} P\left(\frac{\nu}{2}, \frac{b'}{2}\right) - P\left(\frac{\nu}{2}, \frac{a'}{2}\right) &= 1 - 2\delta \\ P\left(\frac{\nu}{2}+1, \frac{b'}{2}\right) - P\left(\frac{\nu}{2}+1, \frac{a'}{2}\right) &= F(b', \nu) - F(a', \nu) \end{cases}$$

Solutions are numerically computed for all the values of ν and for the retained value of $\delta = 30\%$ giving a normalized standard deviation of the unbiased estimator less than 5 %.

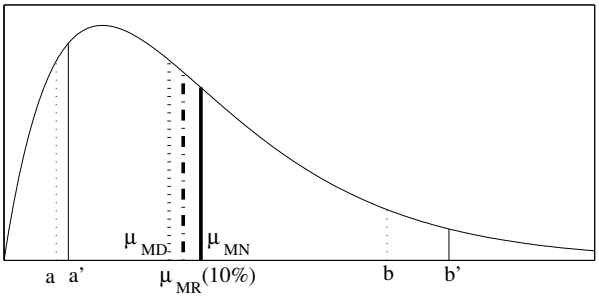

Figure 4: Trimmed values after correction of the trimmed mean estimator. $\mu_{MR}(\alpha)$ is now equal to μ_{MN}.

5. CONCLUSION

Thanks to time-blanking and frequency-blanking, the celestial observation of certain frequency bands that were traditionally highly polluted may finally be explored for scientific purposes. Such blanking methods have proved their efficiency in real-time survey experiments (especially with radar polluters). However, time-blanking assumes very short wide band interferences manifestations and does not take into account permanent or narrow band polluters. These latter change the distribution of the temporal waveform and may have an impact on the threshold.

In practice, front-end analog filters distort the flatness of the expected white noise leading to a reduced RFI blanking efficiency. This work allows a fast and robust estimation of the mean for each single channel resulting in a good estimation of analog filters responses prior to any acquisitions.

REFERENCES

[1] R. Weber, L. Amiaud, A. Coffre, L. Denis, A. Lecacheux, C. Rosolen, C. Viou and P. Zarka, "Digital implementation of a robust radio astronomical spectral analyser: towards IIIZW35 reconquest," in *Proc. EUSIPCO 2004*, Vienna, Austria, September 6-10. 2004, pp. 773776.

[2] M. Abramowitz and I. A. Segun, "Handbook of mathematical functions," *Dover Publications*, New York, 1965.